



# Feasibility of late gadolinium enhancement magnetic resonance imaging to detect ablation lesion gaps in patients undergoing cryoballoon ablation of paroxysmal atrial fibrillation

Tsuyoshi Mishima MD<sup>1,2</sup>  | Koji Miyamoto MD, PhD<sup>1</sup> | Yoshiaki Morita MD<sup>3</sup> |  
 Tsukasa Kamakura MD, PhD<sup>1</sup> | Kenzaburo Nakajima MD<sup>1</sup>  |  
 Kenichiro Yamagata MD, PhD<sup>1</sup> | Mitsuru Wada MD<sup>1</sup> | Kouhei Ishibashi MD, PhD<sup>1</sup> |  
 Yuko Inoue MD, PhD<sup>1</sup> | Satoshi Nagase MD, PhD<sup>1</sup> | Takashi Noda MD, PhD<sup>1</sup> |  
 Takeshi Aiba MD, PhD<sup>1</sup> | Chisato Izumi MD, PhD<sup>1</sup> | Teruo Noguchi MD, PhD<sup>1</sup> |  
 Satoshi Yasuda MD, PhD<sup>1</sup> | Kengo Kusano MD, PhD<sup>1</sup>

<sup>1</sup>Department of Cardiovascular Medicine, National Cerebral and Cardiovascular Center, Suita, Osaka, Japan

<sup>2</sup>Cardiovascular Division, National Hospital Organization, Osaka National Hospital, Osaka, Japan

<sup>3</sup>Department of Radiology, National Cerebral and Cardiovascular Center, Suita, Osaka, Japan

## Correspondence

Koji Miyamoto, Division of Arrhythmia and Electrophysiology, Department of Cardiovascular Medicine, National Cerebral and Cardiovascular Center, Suita, Osaka, Japan.

Email: kojikoji3@gmail.com

## Abstract

**Background:** Although late gadolinium enhancement magnetic resonance imaging (LGE-MRI) allows the identification of lesions and gaps after a cryothermal balloon (CB) ablation of paroxysmal atrial fibrillation (PAF), the accuracy has not yet been well established.

**Methods:** The subjects consisted of 10 consecutive patients who underwent a second ablation procedure among our cohort of 80 patients who underwent LGE-MRI after the CB ablation of PAF. LGE-MRI scar regions were compared with electroanatomical mapping during the second procedure. In the analysis, the unilateral pulmonary vein (PV) antrum was divided into 7 regions.

**Results:** The gap characterization analysis was performed in 140 regions around 40 PVs in total. There were 16 LGE-MRI gaps around 11 PVs (mean  $1.6 \pm 1.4$  gaps/patient) in 7 patients and 14 electrical gaps around 10 PVs in 8 patients (mean  $1.4 \pm 1.1$  gaps/patient). The locations of 13 electrical gaps were well matched to that on the LGE-MRI, whereas the remaining 1 electrical gap had not been predicted on the LGE-MRI. Compared to the electrical gaps in the second procedure, the sensitivity and specificity of the LGE-MRI gaps were 93% (13 LGE-MRI gaps of 14 electrical gaps) and 98% (123 LGE-MRI scars out of 126 electrical scars), respectively.

**Conclusion:** LGE-MRI can accurately localize the lesion gaps after CB ablation of PAF.

## KEYWORDS

ablation, atrial fibrillation, cryothermal balloon, late gadolinium enhancement magnetic resonance imaging, lesion gaps

## 1 | INTRODUCTION

Electrical pulmonary vein (PV) isolation is an effective technique that is used to treat patients with paroxysmal atrial fibrillation (PAF).<sup>1</sup> In recent years, PV isolation by the cryothermal balloon (CB) has been increasingly adopted by electrophysiology laboratories around the world and is comparable to radiofrequency ablation with regard to the efficacy and safety.<sup>2,3</sup> Although the durability of the PV isolation by a CB is higher compared to radiofrequency ablation,<sup>4,5</sup> PV reconnection is still a common observation during repeat procedures in patients with clinical recurrence after CB ablation.<sup>6,7</sup> Previous studies have suggested that late gadolinium enhancement magnetic resonance imaging (LGE-MRI) could visualize the lesion and gaps after ablation procedures, and LGE-MRI shows the relationship between the electrical gaps in the second ablation procedure and the gaps on LGE-MRI.<sup>8,9</sup> However, the accuracy of LGE-MRI is still controversial. Most of these studies analyzed the LGE-MRI after a traditional point-by-point radiofrequency ablation or first-generation CB ablation, and few studies have analyzed that after second-generation CB ablation. The second-generation CB was designed with technical modifications aiming at procedural outcome improvement. The number of injection ports has been doubled and those have been placed more distally on the catheter shaft, resulting in a larger and more uniform zone of freezing on the balloons surface if compared with the previous version.<sup>10</sup> Thus, the lesion sets after second-generation CB ablation are assumed to be wider and more homogeneous than those after the previous modalities, which leads to higher accuracy of LGE-MRI in detecting the ablation lesion gaps. Although LGE-MRI after second-generation CB ablation is reported to be able to visualize the induced ablation lesions,<sup>11,12</sup> the feasibility of LGE-MRI to detect ablation gaps in patients receiving CB ablation has not been well examined. In this study, we examined the accuracy of LGE-MRI in detecting ablation gaps in comparison with the electrophysiological results from the second ablation procedure.

## 2 | METHODS

### 2.1 | Study population

The subjects consisted of 10 consecutive patients who underwent a second ablation procedure among our cohort of 80 patients who underwent LGE-MRI after the CB ablation of PAF from November 2014 to August 2016. All patients gave written informed consent. The study protocol was approved by the hospital's institutional review board, and the study complied with the principles of the Declaration of Helsinki.

### 2.2 | CB catheter ablation

The procedure was performed with patients under deep sedation obtained with dexmedetomidine and propofol. Using the standard Brockenbrough technique, an 8.5 F transeptal sheath (SLO, St. Jude Medical, St. Paul, MN) was introduced into the left atrium (LA) and

exchanged for a 12 F steerable sheath (Flexcath Advance, Medtronic, Minneapolis, MN). Intravenous heparin was administered to maintain an activated clotting time of >300 seconds before the atrial transeptal puncture. A temperature probe (SensiTherm, St. Jude Medical) was placed within the esophagus to monitor the esophageal temperature during the freeze cycle. A spiral mapping catheter (Achieve, Medtronic) was used to advance the 28-mm second-generation CB into the PV for support and to map the PV potentials. After verification of complete sealing at the PV ostium using contrast medium, a freeze cycle of 180 seconds was applied. Additional applications were performed until the PV isolation. A 23-mm CB was not used in any cases. In order to avoid any right phrenic nerve injury, CB applications for the right-sided PVs were applied under monitoring the ipsilateral diaphragmatic compound monitor action potentials during phrenic nerve pacing. CB applications were performed on the order of the left superior PV, left inferior PV, right inferior PV, and right superior PV. All PVs were confirmed to be isolated from the LA by a 20-mm multi-polar ring catheter (Optima, St. Jude Medical) and touch-up ablation was applied when any PVs were not isolated. The ring catheter was also used for obtaining a voltage map of the LA.

### 2.3 | Late gadolinium enhancement magnetic resonance imaging

LGE-MRI was performed 1-3 months after discharge using a 1.5 T scanner (Magnetom Sonata, Siemens, Erlangen, Germany) with a six-channel body array coil using the previously described methods.<sup>8</sup> An intravenous bolus of 0.15 mmol/kg gadolinium contrast (Omniscan, Daiichi Sankyo, Tokyo, Japan) was administered 20 minutes before the three-dimensional (3D) electrocardiographically gated inversion-recovery gradient-echo sequence was applied in the axial orientation. The acquired voxel size was 2.0 × 1.3 × 2.5 mm. Other typical sequence parameters were as follows: repetition time/echo time, 3.5/1.4 ms; flip angle, 10°; bandwidth, 360 Hz/pixel; and inversion time, 300 ms. The scan time for the LGE-MRI sequence was approximately 25 seconds during a breath hold. Cardiac MRIs were reconstructed and analyzed using a workstation (Ziostation2; Ziosoft, Tokyo, Japan). The scar was defined at 2 standard deviations above the normal LA wall tissue mean pixel intensity. The scars were extracted by tracing the hyperenhanced area on a source image, and the 3D volume rendering images of the magnetic resonance angiography overlaid with the PV-LA scar were reconstructed. In the analysis, the unilateral PV antrum was divided into 7 regions—the roof, anterior side, and posterior side of the superior PV, carina region, and the anterior side, posterior side, and bottom of the inferior PV. The overlaid 3D images were analyzed in terms of whether there was enough scar to encircle each PV region.

### 2.4 | Electrophysiological studies in the second ablation procedure

The gaps of the lesions around the PVs were firstly evaluated in the second ablation procedure with a multi-polar ring catheter and

**TABLE 1** Baseline characteristics of the patients and DE-MRI gap characteristics compared with the electrical gaps in the second procedure

Patient	Age, y	Sex	HT	DM	CHA <sub>2</sub> DS <sub>2</sub> -VASc	LAD, mm	Type of recurrent arrhythmia	Time to the 2nd procedure, days	No. of gaps on DE-MRI	Location of gaps on DE-MRI	Location of gaps in the 2nd procedure	Sensitivity	Specificity
1	68	M	Y	N	2	41	PAF	175	3/14	The anterior side of RSPV The carina of RPV The bottom of RIPV	The anterior side of RSPV The carina of RPV The bottom of RIPV	100%	100%
2	61	M	N	N	0	21	PAF	102	2/14	The roof of RSPV The anterior side of RSPV	The roof of RSPV The anterior side of RSPV	100%	100%
3	56	M	N	N	0	46	PAF	609	4/14	The roof of LSPV The roof of RSPV The posterior side of RSPV The bottom of RIPV	The roof of LSPV The roof of RSPV The posterior side of RSPV The bottom of RIPV	100%	91%
4	51	M	Y	N	1	41	PAF	594	0/14	None	None (non-PV foci ablation)	100%	100%
5	68	M	N	N	1	33	PAF	364	0/14	None	The anterior side of RSPV	0%	100%
6	37	M	N	N	0	26	PAF	181	1/14	The roof of LSPV	The roof of LSPV	100%	100%
7	46	M	N	N	0	39	PAF	83	2/14	The posterior side of RIPV The bottom of RIPV	The posterior side of RIPV The bottom of RIPV	100%	100%
8	69	M	N	N	1	37	Atrial tachycardia	42	0/14	None	None (peri-mitral flutter)	100%	100%
9	70	M	Y	Y	3	44	PAF	113	1/14	The roof of LSPV	The roof of LSPV	100%	100%
10	46	M	Y	N	1	41	PAF	102	3/14	The anterior side of RSPV The posterior side of RSPV The roof of LSPV	The anterior side of RSPV The posterior side of RSPV The roof of LSPV	100%	85%
All									16/140			93% (13/14)	98% (123/126)

Gaps detected only on DE-MRI are described in the blue text, and the gap detected only in the second procedure is described in the red text.

DE-MRI, delayed-enhancement magnetic resonance imaging; DM, Diabetes Mellitus; HT, Hypertension; LAD, left atrium diameter; LSPV, left superior pulmonary vein; PAF, paroxysmal atrial fibrillation; PV, pulmonary vein; RIPV, right inferior pulmonary vein; RSPV, right superior pulmonary vein.

3D electro-anatomical mapping system (EAM). The operators were blinded to the results of the LGE-MRI on the initiation of the ablation session. The gaps in the second procedure were compared visually with the gaps of the lesions on the LGE-MRI.

## 2.5 | Statistical analysis

Continuous data are expressed as the mean  $\pm$  SD. The sensitivity of the LGE-MRI was defined as the percentage of electrical gaps in the second procedure that were correctly predicted on the LGE-MRI. The specificity of the LGE-MRI was defined as the percentage of the electrically isolated lesions in the second procedure that were occupied by scar on the LGE-MRI. The statistical analyses were performed using JMP pro 11 software (SAS, Cary, NC).

## 3 | RESULTS

### 3.1 | Patient characteristics and procedural results in the 1st procedure

The patient baseline characteristics were summarized in Table 1. The mean age was  $57 \pm 12$  years old. All patients were male. The mean LA diameter was  $37 \pm 8$  mm. Forty PVs were identified out of a total of 10 patients. Overall, 39 of 40 PVs were successfully isolated using exclusively a 28-mm CB. The mean number of CB applications resulting in a PV isolation were  $1.6 \pm 0.7$ ,  $1.3 \pm 0.9$ ,  $1.6 \pm 1.3$ , and  $1.5 \pm 0.5$ , for the left superior PV, left inferior PV, right superior PV, and right inferior PV, respectively. Real-time recordings of the PV potentials were possible on the spiral catheter during the cryoapplications in

a total of 31PVs (79.5%), including 10 left superior PVs, 8 left inferior PVs, 9 right superior PVs, and 4 right inferior PVs. A touch-up lesion was created in the remaining 1 PV (2.5%) with a cryocatheter on the anterior side of the right superior PV. No complications, including cardiac tamponade or transient phrenic nerve palsy, occurred. The mean total procedural time and total fluoroscopic time were  $148 \pm 48.7$  and  $41.2 \pm 11.1$  minutes, respectively. One patient underwent a second ablation procedure for a recurrence of atrial tachycardia, and the other 9 patients underwent second ablation procedures for recurrence of PAF. The time to the second procedure ranged from 42 to 609 days.

### 3.2 | LGE-MRI gap characteristics

All patients had 4 independent PV ostia. The gap characterization analysis was performed in 140 regions around 40 PVs in total (Table 1). Sixteen LGE-MRI gaps were identified around 11 PVs (mean  $1.6 \pm 1.4$  gaps/patient). The right superior PV had the highest number of gaps (8 gaps in 4 patients), and the left inferior PV the fewest (no gaps). The mean gap length was  $11.6 \pm 3.9$  mm/gap. No PV stenosis was detected on magnetic resonance angiography in this study.

In a comparison between 11 PVs with gaps on the LGE-MRI and 29 PVs without, there was no significant difference in the ablation characteristics in the first procedure, including the number of CB applications resulting in a PV isolation ( $1.72 \pm 1.27$  vs  $1.41 \pm 0.68$ ) or minimum balloon temperature ( $-49.2 \pm 5.5^\circ$  vs  $-49.7 \pm 6.4^\circ$ ). There was a gap on the LGE-MRI in the region of the touch-up ablation, on the anterior side of the right superior PV in patient number 10.

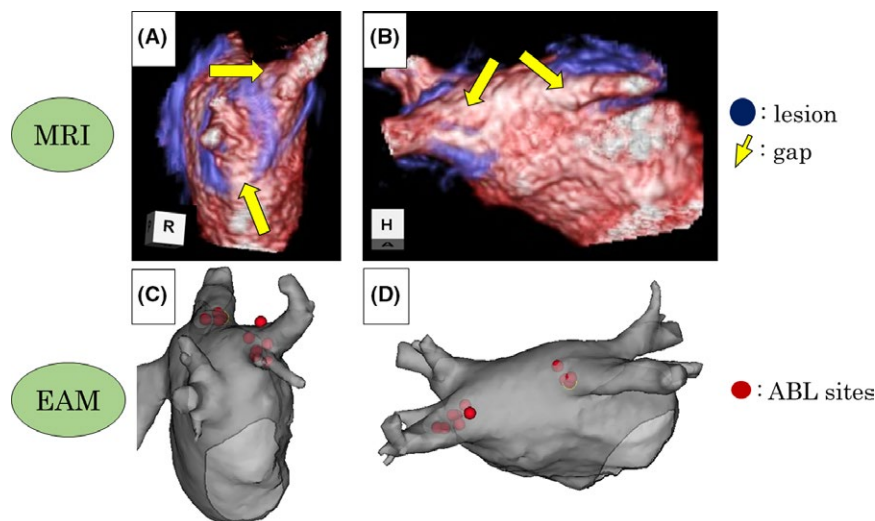


**FIGURE 1** Representative case of electrical gaps in the second ablation procedure accurately predicted on LGE-MRI (patient number 3). A and B, The overlaid images of the three-dimensional reconstructed LGE-MRI and magnetic resonance angiography in the right lateral (A), and cranial (B) views. The site of late gadolinium enhancement is shown as the blue area. There are gaps in the lesion set at the bottom of the right inferior PV, posterior side of the right superior PV, and roof of the right and left superior PVs (arrows). C and D, The electrical gaps to be ablated in the second ablation procedure on the EAM. There are gaps on the posterior side and roof of the right superior PV and roof of the left superior PV (red and green points), and the location of those gaps is well matched to that on the LGE-MRI. The gap in the LGE-MRI on the bottom of the right inferior PV does not correlate with the electrical gap in the second procedure, which indicates the absence of a cardiac muscular sleeve or a nontransmural lesion. EAM, electroanatomical mapping; LGE-MRI, late gadolinium enhancement magnetic resonance imaging; PV, pulmonary vein

### 3.3 | Electrophysiological results in the 2nd procedure

In total, there were 14 electrical gaps around 10 PVs in 8 patients (mean  $1.4 \pm 1.1$  gaps/patient). During the gap ablation, either the activation sequence alternation or elimination of PV potentials was observed using a circular catheter placed in the PV, suggesting that all the identified gaps were correct. The remaining 2 patients had no PV reconstructions: one patient had a non-PV trigger from the right atrium and the other had a peri-mitral flutter. Thirteen electrical gaps had been correctly predicted on the LGE-MRI (Figure 1, Figure S1), including the region of the touch-up ablation, however, the remaining one gap was not. In addition, there were 5 residual potentials in the region of the antrum a little away from the isolation line of the first procedure (2 on the anterior side of the left superior PV, 2 on the posterior side, and 1 at the bottom of the left inferior PV, Figure 2, Figure S2). Ablation was performed until those potentials were diminished.

In the analysis, the unilateral PV antrum was divided into 7 regions -the roof, anterior side, and posterior side of the superior PV, carina region, and the anterior side, posterior side, and bottom of the inferior PV. Among 126 regions in which no electrical gaps were detected in the second ablation procedure, there were also no gaps detected on LGE-MRI in 123 regions. There were 3 regions in which gaps were detected only on the LGE-MRI. Compared to the electrical gaps in the second procedure, the sensitivity and specificity of the LGE-MRI gaps were 93% (13 LGE-MRI gaps of 14 electrical gaps) and 98% (123 LGE-MRI scars out of 126 electrical

scars), respectively (Figure 3, Table 1). There were no low voltage area ( $<0.5$  mV) in the LA in any of the patients.

### 3.4 | Clinical outcomes

After the second ablation procedure, 8 (80%) patients could maintain sinus rhythm during a mean follow-up of 554 days. One patient (patient number 1) with recurrence of PAF after the second procedure underwent a third ablation. There was an electrical gap at the bottom of the right inferior PV, which had been detected both on LGE-MRI and in the second procedure, and there was a focal activation at the antrum of the left PVs. After the ablation of the gap and non-PV foci in the third procedure, he could maintain sinus rhythm during a follow-up of 576 days. The remaining 1 patient (patient number 9), with recurrence of PAF, became asymptomatic while under medication and rejected a third ablation procedure.

## 4 | DISCUSSION

### 4.1 | Main findings—accuracy of LGE-MRI

This study showed that the identification of atrial scarring and gaps by LGE-MRI was feasible and accurate. LGE-MRI accurately predicted 13 of 14 (93%) electrically reconnected sites and 123 of 126 (98%) electrical scars in the second procedure. There were 3 gaps detected only on the LGE-MRI without any correlation to the electrical reconstructions of the PVs. Those gaps on the LGE-MRI probably indicated the absence of any cardiac muscular sleeve or a nontransmural lesion, which was enough to

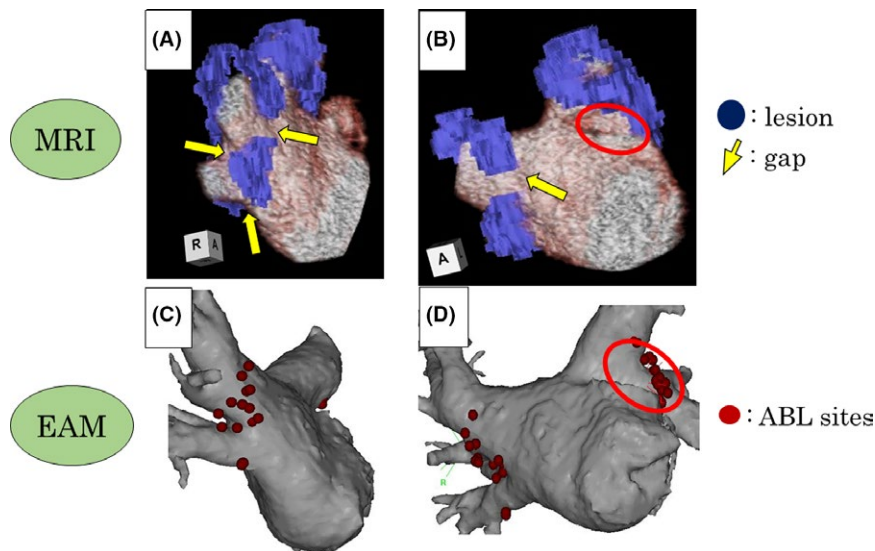


**FIGURE 2** The case with residual potentials in the antrum region beside the ablated area in the first CB ablation procedure (patient number 1). A and B, The overlaid images of the three-dimensional reconstructed LGE-MRI and magnetic resonance angiography in the right lateral view (A), and anterior-posterior view (B). The site of late gadolinium enhancement is shown as the blue area. There are gaps in the lesion set at the bottom of the right inferior PV, carina region of the right PVs, and anterior side of the right superior PV (arrows). C and D, The electrical gaps to be ablated in the second ablation procedure on the EAM. There are gaps on the bottom of the right inferior PV, carina region of the right PVs, and anterior side of the right superior PV (red and yellow points), and the location of those gaps is well matched to that in the LGE-MRI. There are residual potentials to be ablated at the antrum of the left PVs beside the isolation line (red circle). CB, cryothermal balloon; EAM, electroanatomical mapping; LGE-MRI, late gadolinium enhancement magnetic resonance imaging; PV, pulmonary vein

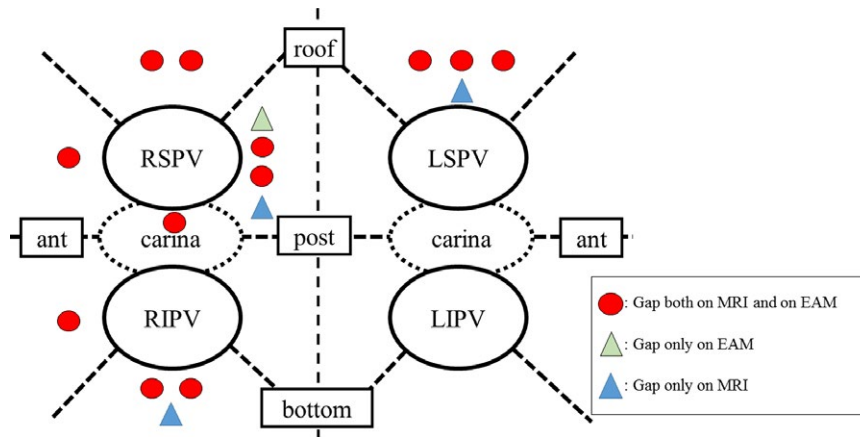


**FIGURE 3** Distribution of the gaps on LGE-MRI and the gaps in the second ablation procedure. The unilateral PV antrum is divided into 7 regions—the roof, anterior side, posterior side of the superior PVs, carina region, and the anterior side, posterior side, and bottom of the inferior PVs. There were 12 electrical gaps in the second procedure accurately predicted on LGE-MRI (red circle). Only 1 gap on the anterior side of the right superior PV was not predicted on the LGE-MRI (green triangle). There were 3 gaps detected only on the LGE-MRI without any correlation to the electrical reconnections of the PV, which indicates the absence of a cardiac muscular sleeve or nontransmural lesions (blue triangle). LGE-MRI, late gadolinium enhancement magnetic resonance imaging; PV, pulmonary vein.

electrically isolate the PV ostium from the LA. Although some reports have questioned the accuracy of LGE-MRI,<sup>9</sup> Halbfass et al. reported that LGE-MRI was able to visualize induced ablation lesions after PV isolation with a CB.<sup>12</sup> Kiuchi et al. highlighted that the lesion formation after CB ablation was wide and homogeneous,<sup>13</sup> and that was why LGE-MRI accurately identified the scar and gaps in this study.

#### 4.2 | Durability of the PVI after the second-generation CB ablation

The number of gaps was 1.6 per patient on the LGE-MRI and 1.4 per patient in the second procedure, which was relatively low compared to that of the previous reports analyzing LGE-MRI after a point-by-point radiofrequency ablation or first-generation CB ablation.<sup>8,9</sup> Ciconte et al. reported that the rate of late PV reconnections was lower following the second-generation CB ablation when compared with contact-force catheter ablation as the index procedure.<sup>5</sup> Giovanni et al. reported that AF recurrence was significantly less frequent in the second-generation CB ablation group with respect to the first-generation CB ablation group.<sup>14</sup> This study was in line with those reports and supports the opinion that second-generation CB ablation makes lesions with a higher durability and less gaps compared to point-by-point radiofrequency ablation or first-generation CB ablation.

#### 4.3 | Possibility of native scar/fibrosis in the LA

There is the possibility that LGE-MRI indicated native scar/fibrosis in the LA, which had existed before the first ablation procedure. LGE-MRI of LA myocardium might not be accurate in detecting ablation lesions in the absence of pre-ablation imaging. McGann et al. investigated the relationship between the LGE-MRI area and volume of the LA.<sup>15</sup> They found that the advanced structural remodeling (LGE-MRI area) was associated with an increased LA volume index. Oakes et al. reported that LGE-MRI associated low voltage area in the LA.<sup>16</sup> In

addition, in human and animal models, heart failure has been reported to increase the atrial fibrosis.<sup>17</sup> Regarding all the cases in this study, the LA, according to the volume index, was not dilated (<50 mL/m<sup>2</sup>) and did not exhibit any low voltage areas in the second procedure, and the patients had no history of heart failure. Therefore, we assumed that the lesion sets visualized by the LGE-MRI in these cases were not native scar/fibrosis, but were ablation-induced scar.

#### 4.4 | Residual potentials of the antrum

Although there were 5 potentials to be ablated, those were located outside the PV isolation line. As Miyazaki et al. reported that the isolated area after a second-generation CB ablation was wide enough, but smaller than that after a circumferential radiofrequency ablation in the EAM analysis,<sup>18</sup> those potentials did not seem to represent a true gap, but instead, the residual potentials of the antrum.

#### 4.5 | Clinical implications

In this study, the LGE-MRI could accurately localize the lesion gaps after the second generation CB ablation of PAF. The clinical implications are considered below:

1. The procedure and fluoroscopy time could be decreased by using the information of the LGE-MRI because the physician could know the location of the lesion gaps before the second ablation procedure.
2. If there is no lesion gap detected on the LGE-MRI the physician could clarify in advance that an ablation strategy focuses on ablation targets other than a PV re-isolation, such as ablating non-PV foci, linear ablation, or a Complex Fractionated Atrial Electrogram ablation. In fact, there were 2 patients with neither lesion gaps detected on the LGE-MRI nor PV reconnections detected in the second procedure. One patient underwent a non-PV foci ablation (triggering

extrasystole from the Supra Vena Cava) and the other patient underwent a mitral isthmus ablation for peri-mitral flutter. The physicians could select those strategies more easily if they knew the information from the LGE-MRI.

#### 4.6 | Limitations

This study has some limitations as follows: The study population was small and a larger prospective study is necessary to confirm our results. The cost-effectiveness of performing an LGE-MRI was unclear. It is reasonable to perform an imaging modality in order to detect PV stenosis because the frequency of the PV stenosis after cryoablation has been reported not to be low.<sup>19</sup> The 1.5 T cardiac MRI has a similar cost to cardiac CT, and MRI is superior to CT in that MRI can detect not only PV stenosis but also the location of lesion gaps. However, performing MRI in all patients after the ablation procedure is controversy because it is unclear whether MRI can be adequately effective to match the increase in the medical expense.

#### 5 | CONCLUSION

This report demonstrated the feasibility of LGE-MRI for accurately localizing the lesion gaps after CB ablation of PAF.

#### CONFLICT OF INTEREST

Authors declare no conflict of interest for this article.

#### ORCID

Tsuyoshi Mishima  <https://orcid.org/0000-0002-9710-6973>

Kenzaburo Nakajima  <https://orcid.org/0000-0002-1279-6558>

#### REFERENCES

- Haissaguerre M, Jais P, Shah DC, et al. Spontaneous initiation of atrial fibrillation by ectopic beats originating in the pulmonary veins. *N Engl J Med*. 1998;339:659–66.
- Kuck KH, Brugada J, Furnkranz A, et al. Cryoballoon or radiofrequency ablation for paroxysmal atrial fibrillation. *N Engl J Med*. 2016;374:2235–45.
- Khoeiry Z, Albenque JP, Providencia R, et al. Outcomes after cryoablation vs. radiofrequency in patients with paroxysmal atrial fibrillation: impact of pulmonary veins anatomy. *Europace*. 2016;18:1343–51.
- Reddy VY, Sediya L, Petru J, et al. Durability of pulmonary vein isolation with cryoballoon ablation: results from the Sustained PV Isolation with Arctic Front Advance (SUPIR) study. *J Cardiovasc Electrophysiol*. 2015;26:493–500.
- Cicconte G, Velagic V, Mugnai G, et al. Electrophysiological findings following pulmonary vein isolation using radiofrequency catheter guided by contact-force and second-generation cryoballoon: lessons from repeat ablation procedures. *Europace*. 2016;18:71–7.
- Heeger CH, Wissner E, Mathew S, et al. Once isolated, always isolated? Incidence and characteristics of pulmonary vein reconduction

after second-generation cryoballoon-based pulmonary vein isolation. *Circ Arrhythm Electrophysiol*. 2015;8:1088–94.

- Miyazaki S, Taniguchi H, Hachiya H, et al. Clinical recurrence and electrical pulmonary vein reconnections after second-generation cryoballoon ablation. *Heart Rhythm*. 2016;13:1852–7.
- Bisbal F, Guiu E, Cabanas-Grandio P, et al. CMR-guided approach to localize and ablate gaps in repeat AF ablation procedure. *JACC Cardiovasc Imaging*. 2014;7:653–63.
- Hunter RJ, Jones DA, Boubertakh R, et al. Diagnostic accuracy of cardiac magnetic resonance imaging in the detection and characterization of left atrial catheter ablation lesions: a multicenter experience. *J Cardiovasc Electrophysiol*. 2013;24:396–403.
- Furnkranz A, Bordignon S, Schmidt B, et al. Improved procedural efficacy of pulmonary vein isolation using the novel second-generation cryoballoon. *J Cardiovasc Electrophysiol*. 2013;24:492–7.
- Mishima T, Miyamoto K, Morita Y, Noda T, Aiba T, Kusano K. Visualization of pulmonary vein-left atrium lesions using delayed-enhancement magnetic resonance imaging after cryothermal balloon catheter ablation: a case report. *HeartRhythm Case Rep*. 2015;1:424–8.
- Halbfass PM, Mitlacher M, Turschner O, Brachmann J, Mahnkopf C. Lesion formation after pulmonary vein isolation using the advance cryoballoon and the standard cryoballoon: lessons learned from late gadolinium enhancement magnetic resonance imaging. *Europace*. 2015;17:566–73.
- Kiuchi K, Fukuzawa K, Takaya T, Nishii T. Homogenous and continuous lesion formation with cryoballoon ablation: delayed-enhancement magnetic resonance imaging analysis. *J Cardiovasc Electrophysiol*. 2016;27:1234–5.
- Giovanni GD, Wauters K, Chierchia GB, et al. One-year follow-up after single procedure cryoballoon ablation: a comparison between the first and second generation balloon. *J Cardiovasc Electrophysiol*. 2014;25:834–9.
- McGann C, Akoum N, Patel A, et al. Atrial fibrillation ablation outcome is predicted by left atrial remodeling on MRI. *Circ Arrhythm Electrophysiol*. 2014;7:23–30.
- Oakes RS, Badger TJ, Kholmovski EG, et al. Detection and quantification of left atrial structural remodeling with delayed-enhancement magnetic resonance imaging in patients with atrial fibrillation. *Circulation*. 2009;119:1758–67.
- Ohtani K, Yutani C, Nagata S, Koretsune Y, Hori M, Kamada T. High prevalence of atrial fibrosis in patients with dilated cardiomyopathy. *J Am Coll Cardiol*. 1995;25:1162–9.
- Miyazaki S, Taniguchi H, Hachiya H, et al. Quantitative analysis of the isolation area during the chronic phase after a 28-mm second-generation cryoballoon ablation demarcated by high-resolution electroanatomic mapping. *Circ Arrhythm Electrophysiol*. 2016;9:e003879.
- Narui R, Tokuda M, Matsushima M, et al. Incidence and factors associated with the occurrence of pulmonary vein narrowing after cryoballoon ablation. *Circ Arrhythm Electrophysiol*. 2017;10:e004588.

#### SUPPORTING INFORMATION

Additional supporting information may be found online in the Supporting Information section at the end of the article.

**How to cite this article:** Mishima T, Miyamoto K, Morita Y, et al. Feasibility of late gadolinium enhancement magnetic resonance imaging to detect ablation lesion gaps in patients undergoing cryoballoon ablation of paroxysmal atrial fibrillation. *J Arrhythmia*. 2019;35:190–196. <https://doi.org/10.1002/joa3.12161>